Biochemical and Biophysical Research Communications 443 (2014) 882–887

Contents lists available at ScienceDirect

Biochemical and Biophysical Research Communications

journal homepage: www.elsevier.com/locate/ybbrc

Targeting of p53 peptide analogues to anti-apoptotic Bcl-2 family proteins as revealed by NMR spectroscopy

Jae-Sun Shin, Ji-Hyang Ha, Seung-Wook Chi *

Medical Proteomics Research Center, KRIBB, Daejeon 305-806, Republic of Korea

ARTICLE INFO

Article history:
Received 7 December 2013
Available online 14 December 2013

Keywords:
p53 Peptide analogue
PMI
pDI
Bcl-2 family proteins
MDM2
NMR spectroscopy
Multi-targeting
Cancer therapy

ABSTRACT

Inhibition of the interaction between the p53 tumor suppressor and its negative regulator MDM2 is of great importance to cancer therapy. The anti-apoptotic Bcl-2 family proteins are also attractive anti-cancer molecular targets, as they are key regulators of apoptotic cell death. Previously, we reported the interactions between the p53 transactivation domain (p53TAD) and diverse members of the anti-apoptotic Bcl-2 family proteins. In this study, we investigated the binding of MDM2-inhibiting p53TAD peptide analogues, p53-MDM2/MDMX inhibitor (PMI) and pDI, with anti-apoptotic Bcl-2 family proteins, Bcl-X_L and Bcl-2, by using NMR spectroscopy. The NMR chemical shift perturbation data demonstrated the direct binding of the p53 peptide analogues to Bcl-X_L and Bcl-2 and showed that the PMI and pDI peptides bind to a conserved hydrophobic groove of the anti-apoptotic Bcl-2 family proteins. Furthermore, the structural model of the Bcl-X_L/PMI peptide complex showed that the binding mode of the PMI peptide is highly similar to that of pro-apoptotic Bcl-2 homology 3 (BH3) peptides. Finally, our structural comparison provided a molecular basis for how the same PMI peptide can bind to two distinct anti-cancer target proteins Bcl-X_L and MDM2, which may have potential applications for multi-targeting cancer therapy.

1. Introduction

Multi-targeting therapy is of significant importance in drug discovery, as it can improve therapeutic efficacy, safety and resistance profiles [1–4]. Single-targeting therapy, where a drug binds specifically to one target molecule, has limited therapeutic efficacy because many diseases are caused by multiple factors. According to the concept of poly-pharmacology, a single drug can bind to more than one target proteins [5]. Despite harmful side effects, these off-target effects of marketed drugs are sometimes beneficial to treatment as seen with anti-cancer multi-kinase inhibitors [5–7]. Thus, it is important to identify the off-target effects of drugs and drug candidates in the field of drug development. Recently, combined drug targeting against multiple apoptotic regulatory proteins has been suggested to provide new opportunities for anti-cancer therapy involving apoptosis induction [6].

p53 is a tumor suppressor protein that mediates cell cycle arrest, DNA repair, apoptosis, and senescence in response to cellular stresses [8,9]. The functional inactivation of p53 has been found in more than 50% of human cancers. MDM2 and MDMX are oncoproteins that negatively regulate the function of p53 via an interaction with the p53 transactivation domain (p53TAD) [10,11]. Thus, blocking the p53TAD-MDM2/MDMX interaction is an important target for cancer therapy [12,13]. Recently, two potent 12-mer p53TAD peptide analogues, termed p53-MDM2/MDMX inhibitor (PMI; TS**F**AEY**W**NL**L**SP) and pDI (LT**F**EHY**W**AQ**L**TS), were selected from a phage displayed peptide library (Fig. 1A) [14–16]. Both PMI and pDI peptides inhibit the interaction between p53TAD and MDM2/MDMX with low nanomolar affinity for both MDM2 and MDMX – two orders of magnitude stronger than the wild-type p53TAD peptide (residues 17–28, ET**F**SDL**W**KL**L**PE) [17] .

The anti-apoptotic Bcl-2 family proteins are key regulators in the mitochondrial apoptosis pathway. Because they are overexpressed in many types of cancers and confer resistance to anti-cancer chemotherapy, Bcl-X_L and Bcl-2 are promising molecular targets for cancer therapy [18–22]. For example, the Bcl-2 family protein inhibitor ABT-737 was found to induce the regression of solid tumors [23], and its derivatives are now under evaluation as anti-cancer therapeutics in clinical trials. Previously, our NMR studies demonstrated that a p53TAD peptide (residues 15–29) binds to diverse anti-apoptotic Bcl-2 family proteins in a manner similar to its interaction with MDM2 [24–27]. Furthermore, we showed that a p53TAD-mimetic MDM2 antagonist, Nutlin-3, binds directly to the anti-apoptotic Bcl-2 family proteins Bcl-X_L, Bcl-2, Bcl-w, and Mcl-1 in an analogous mode [25,28].

To test whether the MDM2-inhibiting p53TAD peptide analogues could target the anti-apoptotic Bcl-2 family proteins, we performed binding experiments for the PMI and pDI peptides with the anti-apoptotic Bcl-2 family proteins Bcl-X_L and Bcl-2 by using

* Corresponding author. Fax: +82 42 879 8596.
E-mail address: swchi@kribb.re.kr (S.-W. Chi).

0006-291X/$ - see front matter © 2013 Elsevier Inc. All rights reserved.
http://dx.doi.org/10.1016/j.bbrc.2013.12.054

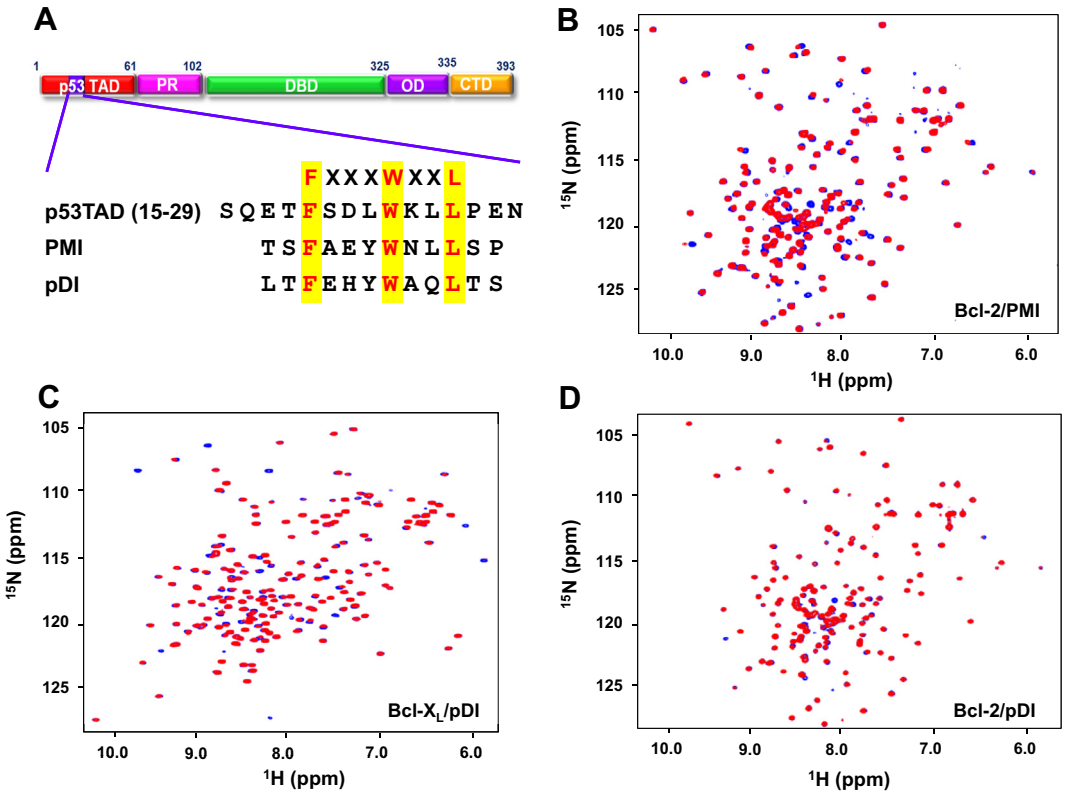

Fig. 1. Binding of p53 peptide analogues to the anti-apoptotic Bcl-2 family proteins. (A) Sequence alignment of the p53TAD peptide analogues, PMI and pDI, with the wild-type p53TAD peptide. (B) The overlaid 2D ^{1}H–^{15}N HSQC spectra for ^{15}N-labeled Bcl-2 in the absence (blue) or presence of the PMI peptide (red). The overlaid 2D ^{1}H–^{15}N HSQC spectra for ^{15}N-labeled Bcl-X_L (C) or Bcl-2 (D) in the absence (blue) or presence of the pDI peptide (red). (For interpretation of the references to color in this figure legend, the reader is referred to the web version of this article.)

NMR spectroscopy. Our results demonstrated direct interactions between peptide analogues and Bcl-X_L and Bcl-2 proteins. The structural model of the Bcl-X_L/PMI peptide complex showed that the PMI peptide binds to Bcl-X_L in a manner analogous to that observed with the pro-apoptotic BH3 peptides. This structural information will contribute to the development of a multi-targeting cancer therapy against two different anti-cancer targets, MDM2 and Bcl-X_L.

2. Materials and methods

2.1. Preparation of proteins and peptides

Truncated Bcl-X_L and Bcl-2 were expressed and purified for NMR experiments as previously reported [25,29,30]. PMI and pDI peptides were chemically synthesized and purified by Peptron Inc as described previously [31,32].

2.2. NMR spectroscopy

All the NMR data were acquired using a Bruker Avance II 800 MHz spectrometer at the Korea Basic Science Institute. The 2D ^{15}N–^{1}H HSQC spectra of Bcl-X_L and Bcl-2 were obtained at 25 °C in the absence or presence of the p53 peptide analogues, pDI and PMI. The NMR samples comprised 90% H_2O/10% D_2O and were prepared in 20 mM sodium phosphate (pH 6.5), 150 mM NaCl, and 1 mM DTT for Bcl-X_L, and 20 mM Tris HCl (pH 7.8), and 5 mM DTT for Bcl-2. For the chemical shift perturbation experiments with the anti-apoptotic Bcl-X_L and Bcl-2 proteins, aliquots of the concentrated peptide (PMI and pDI) stock solution were titrated into the ^{15}N-labeled Bcl-X_L or Bcl-2 and the 2D ^{15}N–^{1}H HSQC spectra were collected at 25 °C. The backbone ^{1}H and ^{15}N resonances of ^{15}N-labeled Bcl-X_L and Bcl-2 were assigned using the previously reported chemical shift assignments [29,33,34]. All the NMR data were processed and analyzed using NMRPipe/NMRDraw [35] and SPARKY software.

2.3. Structure calculation

The structure of the Bcl-X_L/PMI peptide complex was calculated using the program HADDOCK 2.0 [36] in combination with crystallography and NMR system (CNS). Ambiguous interaction restraints (AIRs) were defined on the basis of the NMR chemical shift perturbation data. The "active" residues of Bcl-X_L were defined as those showing a significant chemical shift perturbation value with relatively large per-residue solvent accessibility for either the side-chain or main-chain atoms. All of the surrounding surface residues near the active residues were defined as "passive" residues. Starting from the structures of Bcl-X_L (PDB code: 1BXL) [37] and PMI peptide (PDB code: 3EQS) [15], rigid body energy minimization was performed, leading to 1000 rigid body docking solutions. In terms of intermolecular interaction energy, the 200 lowest structures were selected for rigid body simulated annealing followed by semi-flexible simulated annealing in torsion angle space. Finally, the resulting structures were refined in explicit water by using simulated annealing in Cartesian space. The docking solutions were clustered based on positional root mean square deviation (rmsd) values by using a 3 Å cut-off. The complex models were selected for visualization based on their rmsd from the best energy structure and HADDOCK energy score. Figures of the model were drawn using the PyMOL software package [38].

3. Results and discussion

3.1. Binding of the p53TAD peptide analogues with the anti-apoptotic Bcl-2 family proteins

Our previous studies showed direct binding of the small molecule MDM2 antagonist Nutlin-3 and PMI peptide with the anti-apoptotic Bcl-X_L protein [25,28]. To investigate this further, we examined the binding of the p53 peptide analogues PMI and pDI to Bcl-2 and Bcl-X_L by using NMR spectroscopy. The overlaid 2D ^{1}H–^{15}N HSQC spectra of Bcl-2 and Bcl-X_L in the absence or presence of the PMI or pDI peptide are shown in Fig. 1. Significant chemical shift perturbations in many of the ^{15}N–^{1}H crosspeaks in both Bcl-2 and Bcl-X_L were observed upon the addition of either PMI or pDI peptide, indicating a direct interaction between the pDI and PMI peptides and the anti-apoptotic Bcl-2 family proteins. Interestingly, binding of the PMI and pDI peptides differentially affects the degree of chemical shift changes in the residues within the same hydrophobic binding pocket, in the order of Bcl-X_L/PMI ⩾ Bcl-2/PMI > Bcl-2/pDI ≅ Bcl-X_L/pDI (Fig. 2). In particular, many of Bcl-X_L crosspeaks disappeared upon binding of the PMI peptide because of significant line broadening, indicating fast-to-intermediate exchange on the NMR chemical shift time scale. Although the chemical shift perturbations induced by the PMI peptide were much stronger than those induced by the pDI peptide, the affected residues in Bcl-2 and Bcl-X_L induced by both peptides were similar (Fig. 2), demonstrating that they share the same binding site in Bcl-X_L and Bcl-2. These are consistent with the NMR chemical shift changes seen in Bcl-X_L and Bcl-2 when bound to the wild-type p53TAD peptide (residue 15–29) [25,26].

3.2. Mapping the binding site of the p53TAD peptide analogues on anti-apoptotic Bcl-2 family proteins

The NMR chemical shift perturbations induced by the p53TAD peptide analogues were mapped onto the structures of Bcl-2 and

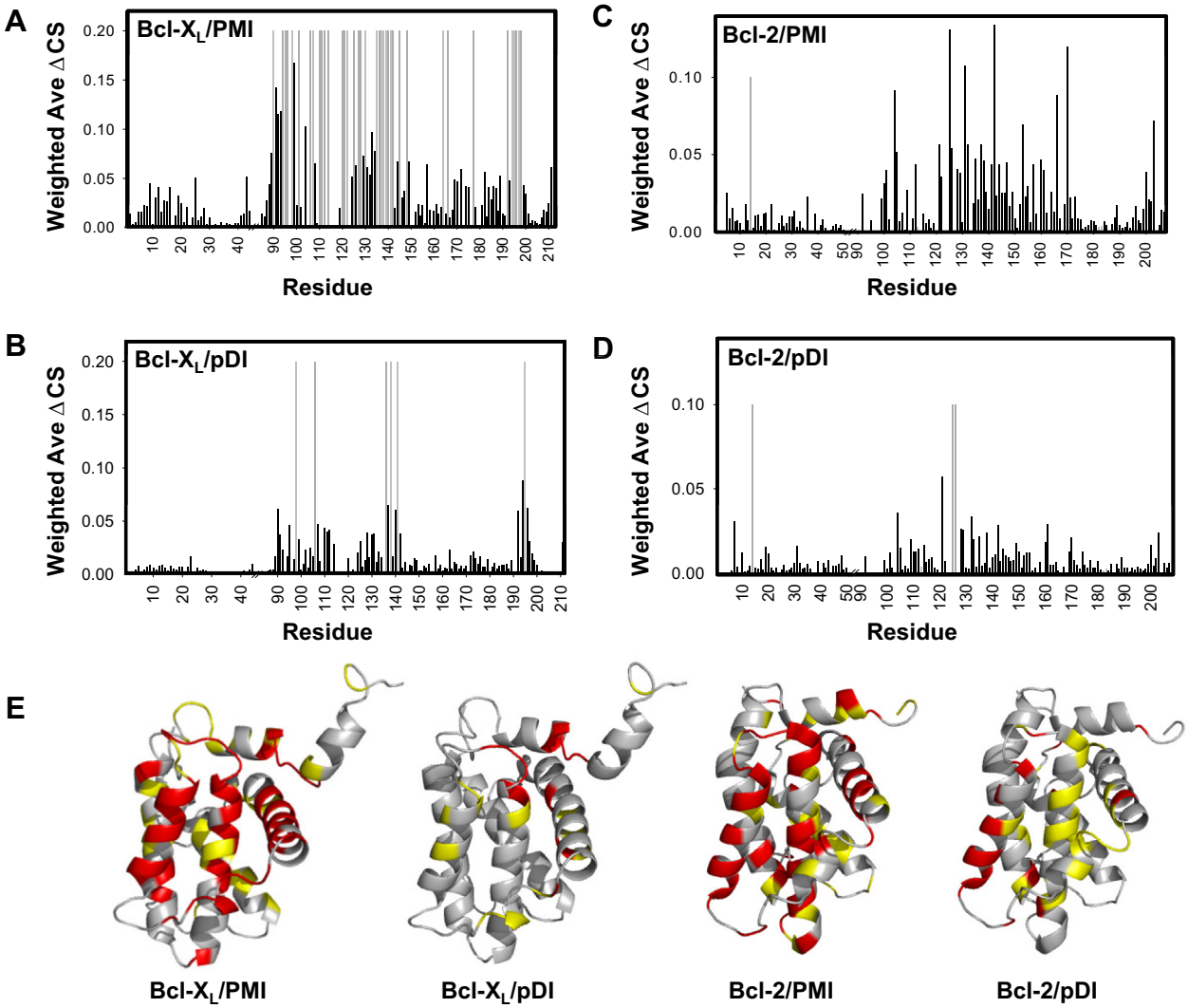

Fig. 2. NMR chemical shift perturbations of the anti-apoptotic Bcl-2 family proteins induced by binding of p53 peptide analogues. NMR chemical shift perturbations of Bcl-X_L residues upon binding of the PMI (A) or pDI (B) peptide. Mapping of chemical shift perturbations of the PMI peptide on the Bcl-X_L structure is based on previous NMR data [25]. NMR chemical shift perturbations of Bcl-2 residues upon binding of the PMI (C) or pDI (D) peptide. Resonances from Bcl-X_L and Bcl-2 that disappeared upon peptide binding are shown as gray bars. (E) Mapping of the binding site for the p53 peptide analogues on Bcl-X_L and Bcl-2 structures. The weighted chemical shift perturbations were calculated by the equation, $\Delta CS = (\Delta^{1}H^{2} + (0.2\Delta^{15}N)^{2})^{0.5}$, in which $\Delta^{1}H$ and $\Delta^{15}N$ are the chemical shift changes on the ^{1}H and ^{15}N dimensions [42]. Bcl-X_L and Bcl-2 residues showing chemical shift changes of $\Delta CS > 0.08$ ppm and $\Delta CS > 0.02$ ppm, respectively, and the residues that disappeared are shown in red. Bcl-X_L and Bcl-2 residues showing the chemical shift changes of 0.025 ppm < ΔCS < 0.08 ppm and 0.01 ppm < ΔCS < 0.02 ppm, respectively, are shown in yellow. (For interpretation of the references to color in this figure legend, the reader is referred to the web version of this article.)

Bcl-X_L to determine the binding site at the three-dimensional level (Fig. 2E). The chemical shift perturbations induced by peptide binding occurred in a hydrophobic groove surrounded by the BH1, BH2, and BH3 domains of Bcl-X_L. This region corresponds to a conserved binding site for the pro-apoptotic BH3 peptides. These results indicate that the p53 peptide analogues PMI and pDI specifically bind to the same site of the anti-apoptotic Bcl-2 family proteins as the p53TAD peptide [26].

3.3. Structural basis for the interaction between Bcl-X_L and the PMI peptide

To understand the structural basis for the interaction between the p53TAD peptide analogues and anti-apoptotic Bcl-2 family proteins, we calculated structural models for the complex between the PMI peptide and Bcl-X_L by using the program HADDOCK 2.0 [26] (Fig. 3A, B). The structural models of the Bcl-X_L/PMI peptide complex are similar to those of Bcl-X_L/p53TAD peptide (residue 15–29) complex [26]. Consistent with the chemical shift perturbation data, the structural model of the Bcl-X_L/PMI peptide complex showed that an amphipathic α-helix of the PMI peptide binds to the long hydrophobic groove in Bcl-X_L (Fig. 3C, D), which corresponds to the binding site for the BH3 peptides of the pro-apoptotic Bcl-2 family proteins Bak, Bad, and Bim (Fig. 3D).

3.4. Structural comparison among the Bcl-X_L/peptide complexes

A detailed structural comparison between the Bcl-X_L/PMI peptide complex and the Bcl-X_L/Bim BH3 peptide complex showed that the PMI peptide binds to Bcl-X_L in a similar manner as the pro-apoptotic BH3 peptide (Fig. 3D). The BH3 peptide-binding groove of Bcl-X_L is composed of four distinct sub-binding sites (*i*, *i* + 4, *i* + 7 and *i* + 11 sites occupied by the side-chains of Ile90, Leu94, Ile97, and Phe101 in the Bim BH3 peptide, respectively). In the Bcl-X_L/PMI peptide complex, three of the four sub-binding sites (*i*, *i* + 4, and *i* + 7 sites) were filled up by the bulky hydrophobic residues, Phe3, Trp7, and Leu10 in the PMI peptide (Fig. 3C, D), although the binding orientation is opposite in the directional sense.

Taken together, the overall binding mode and site of the PMI peptide to Bcl-X_L resemble those of the BH3 peptides to Bcl-X_L. Similar to the pro-apoptotic BH3 peptides, the PMI peptide can compete with the pro-apoptotic BH3 peptides to bind to the same site in Bcl-X_L. This suggests a competitive binding mechanism for the observed tumor killing activity of the PMI peptide [15], where the PMI peptide targets anti-apoptotic Bcl-X_L, rescuing pro-apoptotic Bcl-2 family proteins such as Bak and Bax from complex formation with Bcl-X_L, and thereby inducing mitochondrial apoptosis in cancer cells in a transcription-independent manner.

3.5. Structural insights into the multi-targeting mechanism of the PMI peptide

The structural model of the Bcl-X_L/PMI peptide complex provided a molecular basis for how the same PMI peptide could bind to two distinct proteins MDM2 and Bcl-X_L. Although the overall structures of MDM2 and Bcl-X_L are different (Fig. 4), both contain similar hydrophobic grooves for binding the PMI peptide.

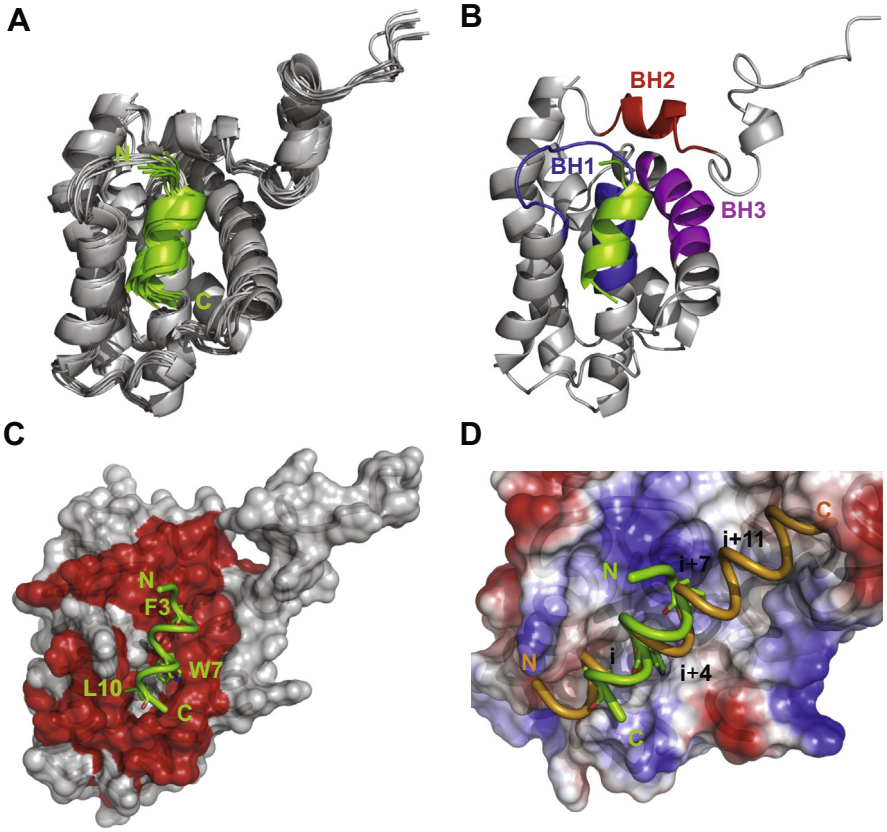

Fig. 3. Structural models of the Bcl-X_L/PMI peptide complex. An ensemble of 8 structural models (A) and the best-energy structural model (B) of Bcl-X_L/PMI peptide complex are shown. Bcl-X_L and PMI peptides are shown in gray and green, respectively. BH1, BH2 and BH3 motifs of Bcl-X_L are labeled. (C) Molecular surface representation of the Bcl-X_L/PMI peptide complex structure. Chemical shift perturbations induced by the PMI peptide on Bcl-X_L are mapped in red on the surface, as defined in Fig. 2E. (D) Superposition of Bcl-X_L/PMI peptide and Bcl-X_L/Bim BH3 peptide complexes (PDB code: 3FDL). PMI and Bim BH3 peptides are colored in green and yellow, respectively. Positive and negative electrostatic potentials on the molecular surface of Bcl-X_L are in blue and red, respectively. (For interpretation of the references to color in this figure legend, the reader is referred to the web version of this article.)

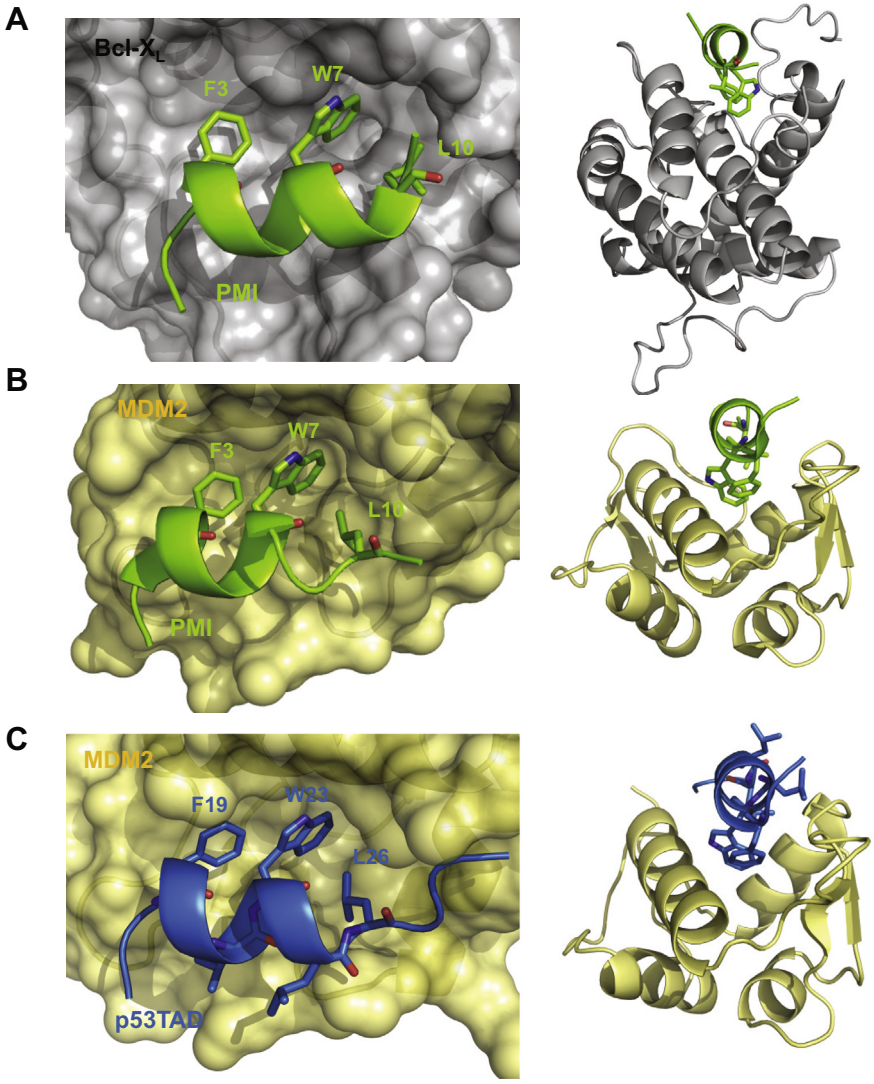

Fig. 4. Mimicry between Bcl-X_L and MDM2 in the binding mode of the PMI peptide. Structural comparison between Bcl-X_L/PMI (A), MDM2/PMI (B), and MDM2/p53TAD peptide (residues 15–29) (C) (PDB code: 1YCR) complexes. PMI and p53TAD peptides are represented as green and blue ribbon models, respectively, and Bcl-X_L and MDM2 are shown in gray and yellow, respectively. The key binding residues from the PMI and p53TAD peptides are labeled. (For interpretation of the references to color in this figure legend, the reader is referred to the web version of this article.)

Interestingly, our structural comparison between the Bcl-X_L/PMI peptide complex (Fig. 4A) and the MDM2/PMI peptide complex (Fig. 4B) [15] revealed a noticeably high similarity in the binding mode of the PMI peptide for MDM2 and Bcl-X_L. First, the amphipathic helical backbone of the PMI peptide closely mimics that of the p53TAD (residues 15–29) peptide bound to MDM2 in both Bcl-X_L/PMI and MDM2/PMI peptide complexes (Fig. 4). The running direction of the PMI and p53TAD peptide backbones is also the same in the MDM2-bound complexes. Second, the hydrophobic side-chains of the key residues Phe3, Trp7, and Leu10, (FXXXWXXL) in the PMI peptide occupy three discrete sub-binding sites in MDM2 and Bcl-X_L filled by Phe19, Trp23, and Leu26 of the p53TAD peptide, respectively (Fig. 4C). This suggests that these three absolutely-conserved hydrophobic residues in the PMI and p53TAD peptides serve as key binding determinants for both MDM2 and Bcl-X_L. This finding agrees well with previous data, where mutations at Phe19, Leu22, and Trp23 of p53TAD disrupted MDM2 binding [39]. Similar to Trp23 in p53TAD, the ring moiety of Trp7 in the PMI peptide fits deeply into the hydrophobic grooves of both MDM2 and Bcl-X_L, making the largest contribution to complex formation.

Both MDM2 and Bcl-X_L are important molecular targets in anti-cancer therapy, as they are essential regulators of apoptotic cell death [18,20,40]. Combined targeting of MDM2 by Nutlin-3a and Bcl-2 by ABT-737 was shown to synergistically induce apoptosis in acute myeloid leukemia, presumably because the inhibition of anti-apoptotic Bcl-2 proteins could increase the apoptogenic effects of MDM2 inhibition [41]. Thus, concomitant inhibition of MDM2 and Bcl-X_L/Bcl-2 may present a multi-targeting therapeutic strategy to induce cancer cell death. The results of the present study suggest that the PMI peptide can also be utilized in such a strategy to inhibit MDM2 and Bcl-X_L/Bcl-2 simultaneously. The structural information from the Bcl-X_L/PMI peptide complex provides information for future structure-based rational design of multi-targeting anti-cancer drugs.

Acknowledgments

This work was supported by the National Research Foundation of Korea (NRF) Grant funded by the Korea government (MSIP) (No. NRF-2011-0016011). This study made use of the NMR facility at Korea Basic Science Institute, which is supported by Advanced

MR Technology Program of the Korean Ministry of Education, Science and Technology.

References

[1] A.L. Hopkins, J.S. Mason, J.P. Overington, Can we rationally design promiscuous drugs?, Curr Opin. Struct. Biol. 16 (2006) 127–136.
[2] X.H. Ma, Z. Shi, C. Tan, Y. Jiang, M.L. Go, B.C. Low, Y.Z. Chen, In-silico approaches to multi-target drug discovery: computer aided multi-target drug design, multi-target virtual screening, Pharm. Res. 27 (2010) 739–749.
[3] J.P. Overington, B. Al-Lazikani, A.L. Hopkins, How many drug targets are there? Nat. Rev. Drug Discovery 5 (2006) 993–996.
[4] Y.J. Lee, J.H. Im, D.M. Lee, J.S. Park, S.Y. Won, M.K. Cho, H.S. Nam, Y.J. Lee, S.H. Lee, Synergistic inhibition of mesothelioma cell growth by the combination of clofarabine and resveratrol involves Nrf2 downregulation, BMB Rep. 45 (2012) 647–652.
[5] A.L. Hopkins, Network pharmacology: the next paradigm in drug discovery, Nat. Chem. Biol. 4 (2008) 682–690.
[6] Y. Dai, S. Grant, Targeting multiple arms of the apoptotic regulatory machinery, Cancer Res. 67 (2007) 2908–2911.
[7] Z. Shi, X.H. Ma, C. Qin, J. Jia, Y.Y. Jiang, C.Y. Tan, Y.Z. Chen, Combinatorial support vector machines approach for virtual screening of selective multi-target serotonin reuptake inhibitors from large compound libraries, J. Mol. Graph. Model 32 (2012) 49–66.
[8] B. Vogelstein, D. Lane, A.J. Levine, Surfing the p53 network, Nature 408 (2000) 307–310.
[9] K.H. Vousden, X. Lu, Live or let die: the cell's response to p53, Nat. Rev. Cancer 2 (2002) 594–604.
[10] J. Momand, G.P. Zambetti, D.C. Olson, D. George, A.J. Levine, The mdm-2 oncogene product forms a complex with the p53 protein and inhibits p53-mediated transactivation, Cell 69 (1992) 1237–1245.
[11] J.D. Oliner, J.A. Pietenpol, S. Thiagalingam, J. Gyuris, K.W. Kinzler, B. Vogelstein, Oncoprotein MDM2 conceals the activation domain of tumour suppressor p53, Nature 362 (1993) 857–860.
[12] D. Alarcon-Vargas, Z. Ronai, p53-Mdm2–the affair that never ends, Carcinogenesis 23 (2002) 541–547.
[13] L.T. Vassilev, B.T. Vu, B. Graves, D. Carvajal, F. Podlaski, Z. Filipovic, N. Kong, U. Kammlott, C. Lukacs, C. Klein, N. Fotouhi, E.A. Liu, In vivo activation of the p53 pathway by small-molecule antagonists of MDM2, Science 303 (2004) 844–848.
[14] M. Liu, C. Li, M. Pazgier, C. Li, Y. Mao, Y. Lv, B. Gu, G. Wei, W. Yuan, C. Zhan, W.Y. Lu, W. Lu, D-peptide inhibitors of the p53-MDM2 interaction for targeted molecular therapy of malignant neoplasms, Proc. Natl. Acad. Sci. U.S.A. 107 (2010) 14321–14326.
[15] M. Pazgier, M. Liu, G. Zou, W. Yuan, C. Li, J. Li, J. Monbo, D. Zella, S.G. Tarasov, W. Lu, Structural basis for high-affinity peptide inhibition of p53 interactions with MDM2 and MDMX, Proc. Natl. Acad. Sci. U.S.A. 106 (2009) 4665–4670.
[16] C. Li, M. Pazgier, C. Li, W. Yuan, M. Liu, G. Wei, W.Y. Lu, W. Lu, Systematic mutational analysis of peptide inhibition of the p53-MDM2/MDMX interactions, J. Mol. Biol. 398 (2010) 200–213.
[17] P.H. Kussie, S. Gorina, V. Marechal, B. Elenbaas, J. Moreau, A.J. Levine, N.P. Pavletich, Structure of the MDM2 oncoprotein bound to the p53 tumor suppressor transactivation domain, Science 274 (1996) 948–953.
[18] M.H. Kang, C.P. Reynolds, Bcl-2 inhibitors: targeting mitochondrial apoptotic pathways in cancer therapy, Clin. Cancer Res. 15 (2009) 1126–1132.
[19] H.R. Kim, Y.M. Heo, K.I. Jeong, Y.M. Kim, H.L. Jang, K.Y. Lee, C.Y. Yeo, S.H. Kim, H.K. Lee, S.R. Kim, E.G. Kim, J.K. Choi, FGF-2 inhibits TNF-alpha mediated apoptosis through upregulation of Bcl2-A1 and Bcl-xL in ATDC5 cells, BMB Rep. 45 (2012) 287–292.
[20] G. Lessene, P.E. Czabotar, P.M. Colman, BCL-2 family antagonists for cancer therapy, Nat. Rev. Drug Discovery 7 (2008) 989–1000.
[21] K.M. Chung, S.W. Yu, Interplay between autophagy and programmed cell death in mammalian neural stem cells, BMB Rep. 46 (2013) 383–390.
[22] B. Qin, B. Xiao, D. Liang, Y. Li, T. Jiang, H. Yang, MicroRNA let-7c inhibits Bcl-xl expression and regulates ox-LDL-induced endothelial apoptosis, BMB Rep. 45 (2012) 464–469.
[23] T. Oltersdorf, S.W. Elmore, A.R. Shoemaker, R.C. Armstrong, D.J. Augeri, B.A. Belli, M. Bruncko, T.L. Deckwerth, J. Dinges, P.J. Hajduk, M.K. Joseph, S. Kitada, S.J. Korsmeyer, A.R. Kunzer, A. Letai, C. Li, M.J. Mitten, D.G. Nettesheim, S. Ng, P.M. Nimmer, J.M. O'Connor, A. Oleksijew, A.M. Petros, J.C. Reed, W. Shen, S.K. Tahir, C.B. Thompson, K.J. Tomaselli, B. Wang, M.D. Wendt, H. Zhang, S.W. Fesik, S.H. Rosenberg, An inhibitor of Bcl-2 family proteins induces regression of solid tumours, Nature 435 (2005) 677–681.
[24] N. Bharatham, S.W. Chi, H.S. Yoon, Molecular basis of Bcl-X(L)-p53 interaction: insights from molecular dynamics simulations, PLoS ONE 6 (2011) e26014.
[25] J.H. Ha, E.Y. Won, J.S. Shin, M. Jang, K.S. Ryu, K.H. Bae, S.G. Park, B.C. Park, H.S. Yoon, S.W. Chi, Molecular mimicry-based repositioning of nutlin-3 to anti-apoptotic Bcl-2 family proteins, J. Am. Chem. Soc. 133 (2011) 1244–1247.
[26] H. Xu, H. Ye, N.E. Osman, K. Sadler, E.Y. Won, S.W. Chi, H.S. Yoon, The MDM2-binding region in the transactivation domain of p53 also acts as a Bcl-X(L)-binding motif, Biochemistry 48 (2009) 12159–12168.
[27] J.H. Ha, J.S. Shin, M.K. Yoon, M.S. Lee, F. He, K.H. Bae, H.S. Yoon, C.K. Lee, S.G. Park, Y. Muto, S.W. Chi, Dual-site interactions of p53 protein transactivation domain with anti-apoptotic Bcl-2 family proteins reveal a highly convergent mechanism of divergent p53 pathways, J. Biol. Chem. 288 (2013) 7387–7398.
[28] J.S. Shin, J.H. Ha, F. He, Y. Muto, K.S. Ryu, H.S. Yoon, S. Kang, S.G. Park, B.C. Park, S.U. Choi, S.W. Chi, Structural insights into the dual-targeting mechanism of Nutlin-3, Biochem. Biophys. Res. Commun. 420 (2012) 48–53.
[29] A.M. Petros, A. Medek, D.G. Nettesheim, D.H. Kim, H.S. Yoon, K. Swift, E.D. Matayoshi, T. Oltersdorf, S.W. Fesik, Solution structure of the antiapoptotic protein bcl-2, Proc. Natl. Acad. Sci. U.S.A. 98 (2001) 3012–3017.
[30] D.H. Lee, J.H. Ha, Y. Kim, K.H. Bae, J.Y. Park, W.S. Choi, H.S. Yoon, S.G. Park, B.C. Park, G.S. Yi, S.W. Chi, Interaction of a putative BH3 domain of clusterin with anti-apoptotic Bcl-2 family proteins as revealed by NMR spectroscopy, Biochem. Biophys. Res. Commun. 408 (2011) 541–547.
[31] B.R. Kang, H. Kim, S.H. Nam, E.Y. Yun, S.R. Kim, M.Y. Ahn, J.S. Chang, J.S. Hwang, CopA3 peptide from *Copris tripartitus* induces apoptosis in human leukemia cells via a caspase-independent pathway, BMB Rep. 45 (2012) 85–90.
[32] E. Lee, K.W. Jeong, J. Lee, A. Shin, J.K. Kim, J. Lee, D.G. Lee, Y. Kim, Structure-activity relationships of cecropin-like peptides and their interactions with phospholipid membrane, BMB Rep. 46 (2013) 282–287.
[33] A.V. Follis, J.E. Chipuk, J.C. Fisher, M.K. Yun, C.R. Grace, A. Nourse, K. Baran, L. Ou, L. Min, S.W. White, D.R. Green, R.W. Kriwacki, PUMA binding induces partial unfolding within BCL-xL to disrupt p53 binding and promote apoptosis, Nat. Chem. Biol. 9 (2013) 163–168.
[34] A.M. Petros, S.W. Fesik, E.T. Olejniczak, ^{1}H, ^{13}C and ^{15}N resonance assignments of a Bcl-xL/bad peptide complex, J. Biomol. NMR 32 (2005) 260.
[35] F. Delaglio, S. Grzesiek, G.W. Vuister, G. Zhu, J. Pfeifer, A. Bax, NMRPipe: a multidimensional spectral processing system based on UNIX pipes, J. Biomol. NMR 6 (1995) 277–293.
[36] C. Dominguez, R. Boelens, A.M. Bonvin, HADDOCK: a protein-protein docking approach based on biochemical or biophysical information, J. Am. Chem. Soc. 125 (2003) 1731–1737.
[37] M. Sattler, H. Liang, D. Nettesheim, R.P. Meadows, J.E. Harlan, M. Eberstadt, H.S. Yoon, S.B. Shuker, B.S. Chang, A.J. Minn, C.B. Thompson, S.W. Fesik, Structure of Bcl-xL–Bak peptide complex: recognition between regulators of apoptosis, Science 275 (1997) 983–986.
[38] W.L. DeLano, The PyMOL Molecular Graphics System, PyMOL, DeLano Scientific, 2002.
[39] S.M. Picksley, B. Vojtesek, A. Sparks, D.P. Lane, Immunochemical analysis of the interaction of p53 with MDM2;–fine mapping of the MDM2 binding site on p53 using synthetic peptides, Oncogene 9 (1994) 2523–2529.
[40] L.T. Vassilev, MDM2 inhibitors for cancer therapy, Trends Mol. Med. 13 (2007) 23–31.
[41] K. Kojima, M. Konopleva, I.J. Samudio, W.D. Schober, W.G. Bornmann, M. Andreeff, Concomitant inhibition of MDM2 and Bcl-2 protein function synergistically induce mitochondrial apoptosis in AML, Cell Cycle 5 (2006) 2778–2786.
[42] R. Stoll, C. Renner, S. Hansen, S. Palme, C. Klein, A. Belling, W. Zeslawski, M. Kamionka, T. Rehm, P. Muhlhahn, R. Schumacher, F. Hesse, B. Kaluza, W. Voelter, R.A. Engh, T.A. Holak, Chalcone derivatives antagonize interactions between the human oncoprotein MDM2 and p53, Biochemistry 40 (2001) 336–344.